sciendo INTERNATIONAL JOURNAL ON SMART SENSING AND INTELLIGENT SYSTEMS

Research article | DOI: 10.2478/ijssis-2024-0020 Issue 1 | Vol. 17 (2024)

Investigation of torque and sensitivity analysis of a two-phase hybrid stepper motor

Mohammadreza Hojati[1,*], Amir Baktash[2] and Subhas C. Mukhopadhyay[1]

[1]Department of Mechanical Engineering (Mechatronics), School of Engineering, Faculty of Science and Engineering, Macquarie University, Sydney, Australia

[2]Smart Microgrid Research Center, Najafabad Branch, Islamic Azad University, Najafabad, Iran

*E-mail: mohammadreza.hojati@hdr.mq.edu.au

Received for publication May 24, 2024.

Abstract

Stepper motors are extensively used in various automated systems, notably hybrid stepper motors (HSMs), renowned for their high torque density. Optimizing and improving their performance and torque density is highly beneficial. The first step in motor optimization is to perform a sensitivity analysis to identify the parameters most significantly affecting motor performance and torque density. Using Ansys Maxwell, a finite element method (FEM) software, we modeled and analyzed a commercially available HSM. After validating the computer model's accuracy, we investigated the motor's sensitivity to various parameters and discussed their effects on performance. Our findings highlight the significance of parameters such as air gap, magnet diameter, wire-turn numbers in the coils, and the shapes of the rotor and stator teeth in influencing HSM sensitivity—conversely, factors like magnet height and stator pole thickness exhibit negligible impact on motor performance.

Keywords

finite element method, hybrid stepper motor, sensitivity analysis, torque analysis, holding torque

I. Introduction

Stepper motors are recognized as synchronous motors ideally suited for low-speed, high-torque applications that demand precise position control. This is attributed to their characteristic step-by-step rotation, enabling them to lock into each step and maintain their position without interruption [1].

Based on their structure, stepper motors come in three main types: variable reluctance, permanent magnet, and hybrid. Variable reluctance stepper motors feature a lightweight, non-magnetized toothed rotor, facilitating rapid responses and accelerations, making them ideal for applications requiring swift reactions [1]. Permanent magnet stepper motors share similarities with variable reluctance types but possess a magnetized rotor with fewer teeth. Hybrid stepper motors (HSMs), a combination of the two, offer the capability to deliver high torques at low speeds, owing to their rotor structure comprising both permanent magnets and toothed metal. These characteristics have rendered HSMs increasingly prevalent, emerging as the preferred choice across various applications.

Stepper motors are very common and find extensive use across a myriad of applications, including positioning [2, 3], robotics [4–9], and even visual instruments such as cameras [10]. Based on this, there are many articles about stepper motors, but most of them are about presenting different methods for speed and position controlling in these actuators. Jenkins et al. [11] have introduced a method for optimizing the balance between the magnets in the rotor and the coils in the stator to obtain the desired static torque. They could calculate the motor's parameters for different situations and the rotor's different positions from the stator by

preparing the motor‘s equivalent magnetic circuit. Based on these parameters they made their desired changes to the motor‘s structure. Jung et al. [12] also have introduced a method for optimizing static torque in permanent magnet stepper motors. They analyzed the HSM with a few selected parameters such as teeth form and the number of wire-turns in each stator pole using the 3D finite element method (FEM) along with the design of experiments (DOE) method. Kosaka and Matsui [13] also performed a nonlinear magnet analysis in a HSM. Their aim in this paper was to introduce a method for increasing 3D FEM analysis speed while FEM itself is significantly time-consuming.

Matsui et al. [14] have presented a method to analyze continuous torque in HSMs using its magnetic circuit. They divided the air gap between rotor and stator teeth into five separate spaces and calculated permeability for these sections and the motor‘s continuous torque using these calculations. Rao and Prasad [15] have analyzed HSM’s torque using its equivalent magnetic circuit along with 2D FEM. They used the sectioning method to divide the space between the teeth of the rotor and the stator into five sections to analyze it easier.

Stuebig and Ponick [16] have achieved a faster method to calculate the stepper motor parameters by combining FEM and the analysis method. They first prepared the motor‘s equivalent magnetic circuit, then with the use of 2D FEM, they calculated the magnetic permeability for each element. And after the calculation of the required parameters, they could achieve the motor‘s torque. Kang and Lieu [17] have proposed a parametric magnetic model for a 5-phase HSM and analyzed that along with 2D FEM to calculate its torque. Lim et al. [18] also have used FEM, equivalent magnetic circuit, and neural network to estimate and calculate unknown parameters for a 5-phase stepper motor.

A lot of research has been done on different methods to control stepper motors. Besides, several new geometries for stepper motors have been represented by researchers. Bendjedia et al. [19] could estimate speed and rotor position in a HSM without using any mechanical sensor but by the use of digital signal processing and Kalman filter. Lin and Zheng [20] also could control a HSM’s torque practically and in simulation without the usage of any sensor and just by using digital signal processing. Butcher et al. [21] have proposed a new electrical model usable in stepper motor control applications.

Le-Huy et al. [22] have proposed a comprehensive model that can be used in MATLAB- SIMULINK to calculate desired parameters using this environment. Yazdani et al. [23] also have presented a new PID controller that can improve motor speed tracking. Lu et al. [24] have accomplished the designing and fabrication of a novel stepper motor with permanent magnets in its stator structure. Kavitha and Umamaheswari [25] also have designed and analyzed a novel disk-type stepper motor. Last but not least, Hojati et al. [26, 27] have designed three new structures that have increased HSMs torque density dramatically.

Despite this wealth of research, limited attention has been directed toward investigating the behavior of HSMs under varying conditions and their sensitivity to different parameters. Hence, this study aims to address this gap comprehensively. Section 2 outlines the modeling of a real HSM, followed by an analytical study in Section 3. Finally, Section 4 delves into the motor’s sensitivity to different parameters.

II. Modeling a real HSM

To investigate different parameters of a HSM, a two-phase HSM was chosen and modeled (Figure 1). The specifications and dimensions of this motor are shown in Table 1.

This stepper motor has a stator with eight poles and a rotor consisting of two half-rotors which are mounted together with a 3.6° mechanical phase difference. Since some of the motor specifications such as the magnet, rotor, and stator materials were unknown, a trial-and-error method had to be used. So, at first, a few different coil currents were applied to one of the stator phases, and the motor holding torque was calculated. The testbed to measure this torque is shown in Figure 2.

Since only one phase of the motor is excited, the stepper motor remains locked in its position and the holding torque is measurable. To calculate the produced holding torque in this state, different weights were placed on a 60 mm arm coupled with the motor shaft. The weights for each test mode were added until the motor was released from its locked position. In each case, a digital balance was used to measure the weights. Finally, the motor torque was assessed with this data. Table 2 shows the results of this experiment.

Using the obtained data, a computer model of the motor in Ansys Maxwell was designed and analyzed with 1.5 A coil excitation. The results of this simulation were similar to practical tests with a good approximation that can be seen in Figure 3, and the simulated motor is illustrated in Figure 4.

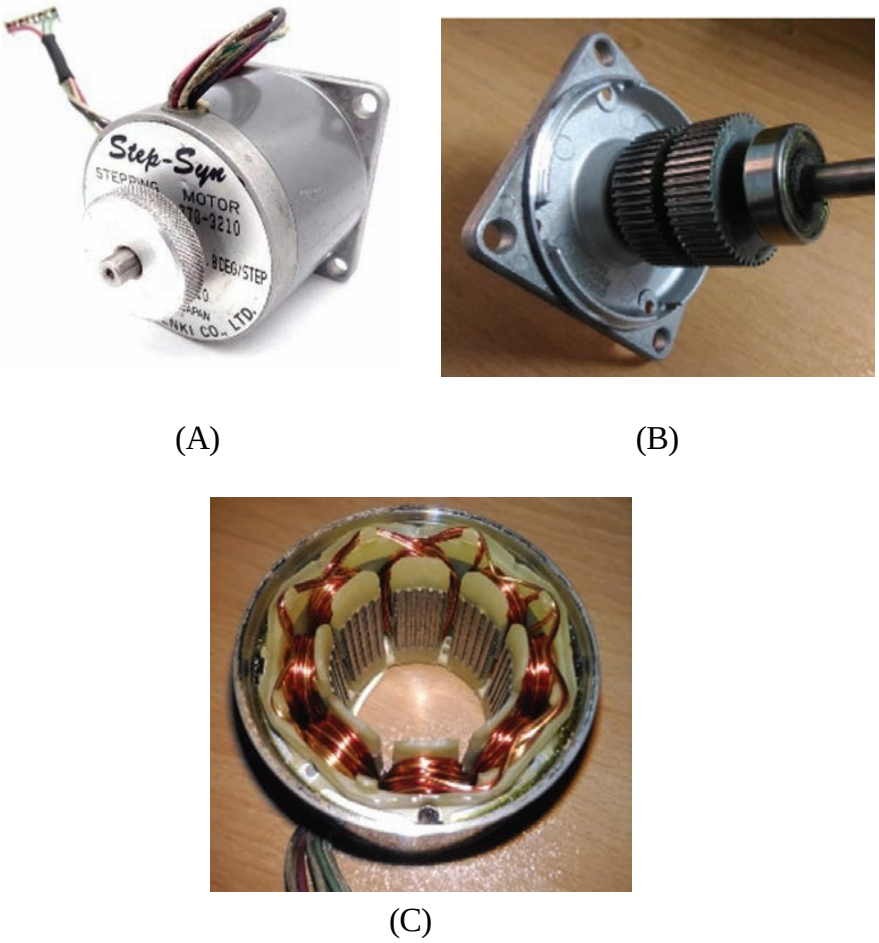

Figure 1: A two-phase HSM, (A) Whole motor, (B) Rotor, and (C) Stator [28]. HSM, hybrid stepper motor.

After preparing the computer model, the actual motor and the modeled motor performances were measured and compared at several points to ensure the precision of all motor parameters and consequently the simulation accuracy. The results confirmed the accuracy of the simulated model. Figure 3 shows the output holding torque of the simulated model in Ansys Maxwell software for the states corresponding to Table 2.

III. Analytical study of the motor

By modeling the motor to study it analytically, the motor's specifications and output torque can be calculated quickly and accurately. This method is very useful for studying motor sensitivity to its various parameters. According to the papers [14, 15], the magnetic permeability of the air gap between the rotor and stator teeth is divided into five zones (Figure 5). Based on the parameters of these five regions and the applied current, the output voltage, flux linkage, and motor torque can be calculated.

Based on Eqs (1)–(5), the permeances P1 to P5 can be calculated [14]:

$$P_1 = h\mu_0 \frac{t-x}{g} \quad (1)$$

$$P_2 = h\mu_0 \frac{2}{\pi} ln\left(1+\frac{\pi x}{2g}\right) \quad (2)$$

$$P_3 = h\mu_0 \frac{1}{\pi} ln\left(\frac{g+2d-\frac{\pi x}{2}}{g+\frac{\pi x}{2}}\right) \quad (3)$$

Table 1: Motor specifications [28]

Motor outer diameter	56.5 mm
Motor body height	52 mm
Stator outer diameter	54.1 mm
Stator inner diameter	30 mm
Number of teeth in each stator pole	5
Stator teeth depth	1.25 mm
Stator height	23 mm
Air gap	0.1 mm
Rotor outer diameter	29.8 mm
Each half-rotor height	10 mm
Distance between two half-rotors	3 mm
Number of teeth in each half-rotor	50
Rotor teeth depth	1.5 mm
Magnet diameter	20.8 mm
Magnet height	13 mm
Number of wire-turns per coil	32
Wire diameter	0.6 mm
Stator and rotor material	Steel 1,008
Magnet material	NdFe35 (1.3 T)
Stator and rotors teeth fillet radius	0.125 mm
Maximum nominal current	3A
Angle per step	1.8°
Rotor and stator teeth angle (pitch)	7.2°
Rotor and stator teeth width	3.6°(0.94 mm)
Stator pole thickness	2 mm

$$P_4 = h\mu_0 \frac{2}{\pi} ln\left(\frac{g+2d}{g+2d+\frac{\pi x}{2}}\right) \quad (4)$$

$$P_5 = h\mu_0 \frac{s-x-\frac{4d}{\pi}}{g+2d} \quad (5)$$

In the above equations, h is the rotor and stator height, μ_0 is the vacuum magnetic permeability coefficient, and t is the slot thickness; x is the amount of nonalignment between rotor and stator teeth. The parameter g is the air gap length and d is the depth of the rotor and stator teeth. These dimensions are listed in Table 3. The total permeance of each pole can be calculated from Eq. (6). In this equation, Z_s is the number of teeth per stator pole, and it is five for this motor:

Table 2: Stepper motor experiment results [28]

Current [A]	Weights mass [g]	Torque [mN/m]
1.05	218	130.8
1.53	297	178.2
1.96	373	223.8
2.35	433	259.8
2.73	477	286.2

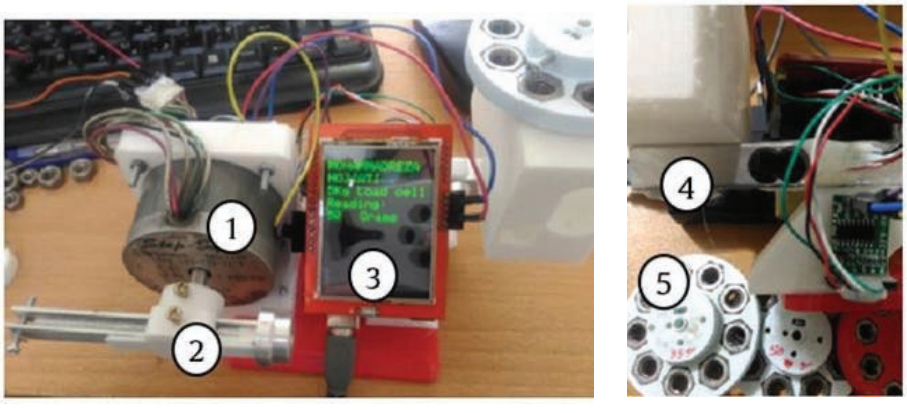

(A) (B)

Figure 2: Stepper motor testbed, (A) Front view, (B) Back view, 1: Stepper motor, 2: Weights carrier arm, 3: Arduino and LCD shield, 4: Load cell, 5: Weights [28].

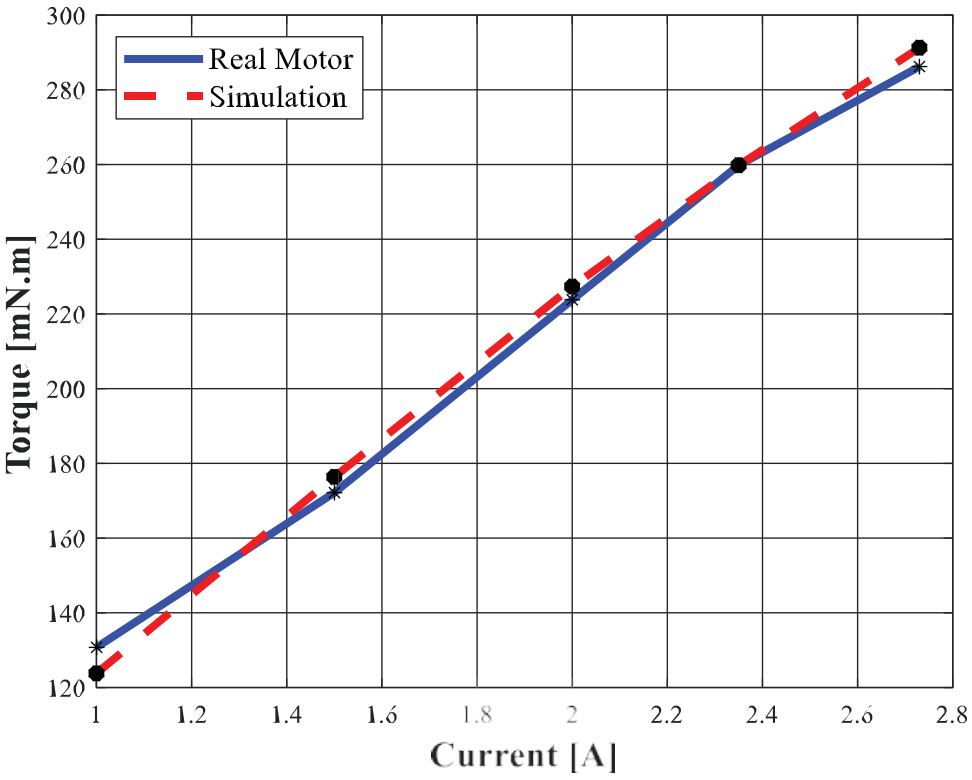

Figure 3: Real motor and simulated model output torque [28].

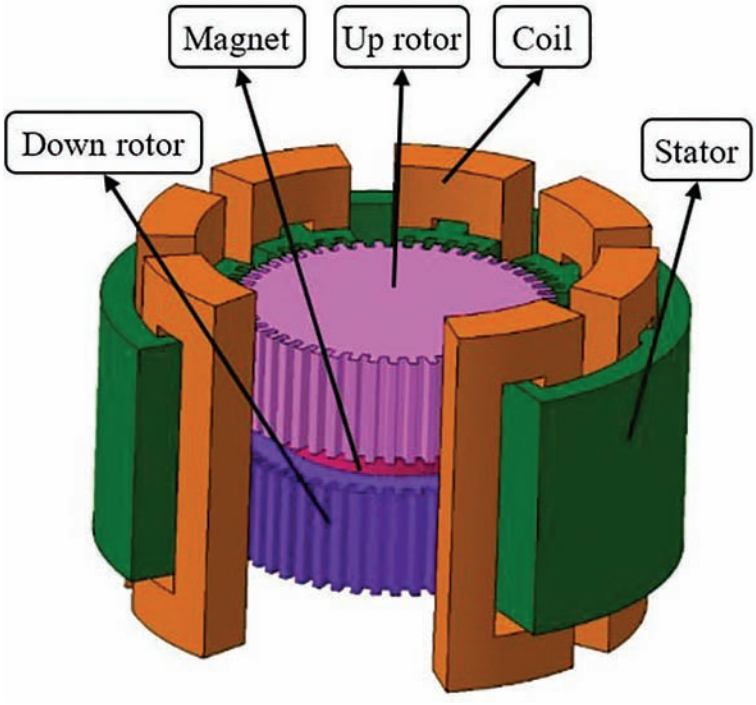

Figure 4: HSM computer model. HSM, hybrid stepper motor.

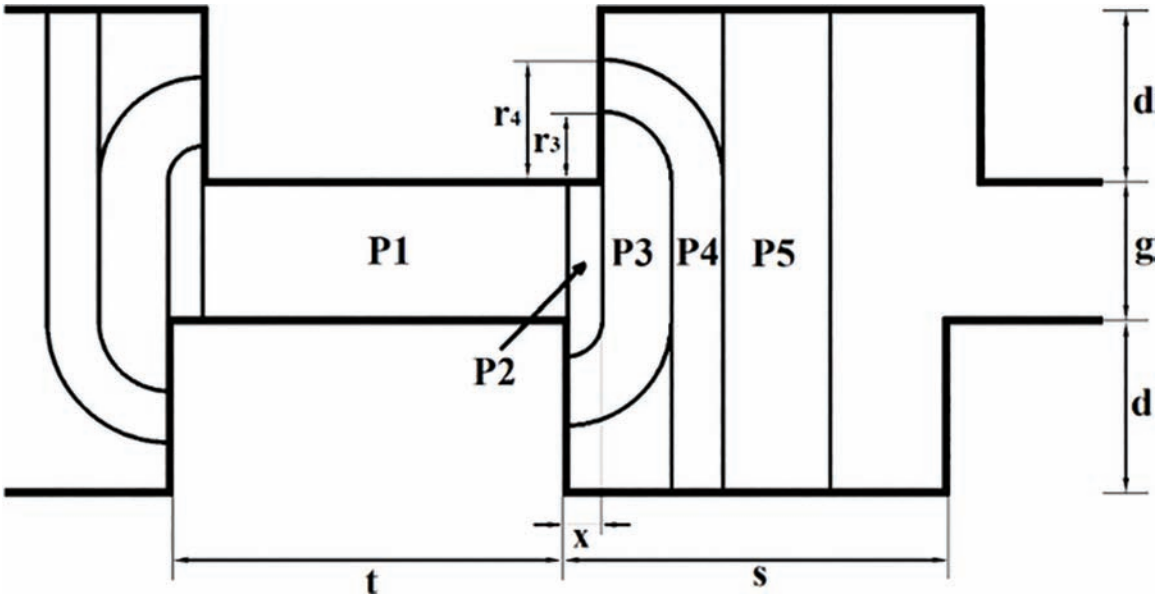

Figure 5: Linearized tooth to tooth arrangement and flux tubes [14, 15].

$$P_t = Z_s[P_1 + 2(P_2 + P_3 + P_4) + P_5] \quad (6)$$

The torque waveform created by each tooth is sinusoidal over the electrical angle (θ). The Eq. (7) is used to calculate this angle. In this equation, Z_r is the number of rotor teeth which is 50 for this motor and θ_m is the mechanical angle:

$$\theta = Z_r \theta_m \quad (7)$$

Eqs (8) and (9) according to Figure 6, are used to calculate the flux linkage in α and β phases. In these equations, N_s is the number of wire-turns per stator winding, i_α and i_β are the excitation currents of α and β phases, respectively, and F_m is the equivalent *mmf* of the permanent magnet:

$$\psi_\alpha = 2(P_\alpha + P_\alpha^{'})N_s^2 i_\alpha + (P_\alpha - P_\alpha^{'})N_s F_m \quad (8)$$

$$\psi_\beta = 2(P_\beta + P_\beta^{'})N_s^2 i_\beta + (P_\beta - P_\beta^{'})N_s F_m \quad (9)$$

Based on the values calculated in the above equations, Eq. (10) determines the torque genere ated by the motor. In Eq. (6), the values of induct-ances L_α and L_β are calculated according to Eqs (11) and (12).

To calculate the static torque waveform for an electric angle period ($\theta = 0 – 2\pi$), the above equations and MATLAB were used. In Table 3, the parameters used in this analysis are outlined.

$$T = Z_r\left(\frac{1\partial L_\alpha}{2\partial\theta} i_\alpha^2 + \frac{1\partial L_\beta}{2\partial\theta} i_\beta^2 + i_\alpha \frac{\partial \psi_\alpha}{\partial\theta} + i_\beta \frac{\partial \psi_\beta}{\partial\theta}\right) \quad (10)$$

$$L_\alpha = 2(P_\alpha + P_\alpha^{'})N_s^2 \quad (11)$$

$$L_\beta = 2(P_\beta + P_\beta^{'})N_s^2 \quad (12)$$

Figure 7 also shows the comparison of the torque curve of the numerical simulation and analytical model. The difference in the graphs is due to the sim-plifications used in analytical equations.

IV. Motor sensitivity analysis using 3D FEM software

Many parameters influence the design of a step-per motor, with varying degrees of impact on its final performance. While some parameters have minimal effects, others significantly alter motor behavior with slight adjustments. This section examines key param-eters in HSMs. The methodology involves keeping all

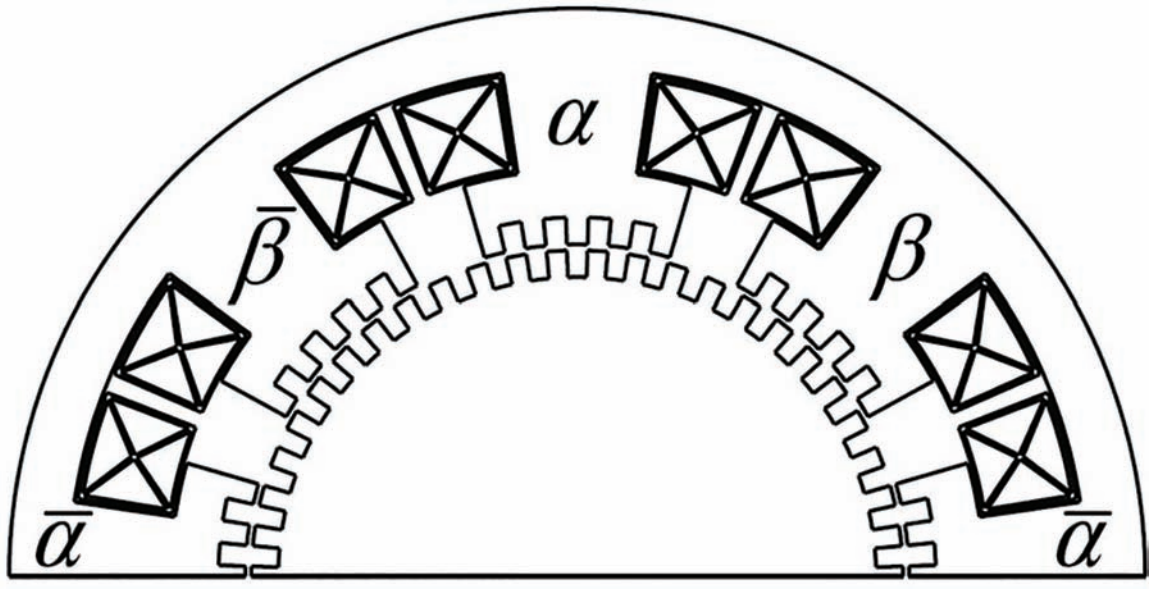

Figure 6: Construction of a two-phase hybrid stepping motor [14].

Table 3: The motor parameters

Absolute permeability	μ_0	$4\pi \times 10^{-7}$ H/m
Slot thickness	t	0.939 mm
Air gap length	g	0.1 mm
Rotor and stator teeth depth	d	1.375 mm
Tooth thickness	s	0.939 mm
Number of teeth per stator pole	Z_s	5
Number of rotor teeth	Z_r	50
Number of wire-turns per stator winding	N_s	32
Excitation current	i	1.5 A
Rotor height	h	20 mm

parameters in the motor model constant except for the one under investigation. This specific parameter is varied from a minimum to a maximum value, and its effects on the motor's output torque are measured. Through this approach, the motor's sensitivity to each parameter can be comprehensively analyzed.

Meshing is very important in finite element analysis; therefore, different meshes were used in this step. The meshing method and the size of the meshes for each zone were based on their influence on the magnetic flux path and the purpose of the analysis. Figure 8 illustrates a sample meshing used for this analysis. In this picture, the parts of the stator that are attracted by the rotor have the finest meshes, and the parts of it that do not have any significant influence on the magnetic flux, have larger meshes.

a. Magnet height

The strength of a magnet depends on its material and its dimensions. Besides, the magnitude of the magnetic field produced by the magnets depends only on its material; and the magnets' dimensions do not have any influence on its magnitude. The magnet's dimensions only influence the magnetic flux density around it. In this motor, a cylindrical magnet is used; as the magnet height increases, it appears that the power of the motor and thus, the produced torque should increase. However, as can be seen in Figure 9, the results obtained by the software show that this conclusion is incorrect and the magnet height has no specific and important effect on motor performance, therefore, the motor has no sensitivity to this parameter. In Figures 9 and 10, all the parameters are the same as in Table 1 except for the magnet height. As shown in Figure 10, the cause of this insensitivity is how magnetic flux is distributed in the motor. As the magnet height increases or decreases, the magnetic flux distribution and its density on the teeth and the air gap do not change; therefore, the motor torque remains constant. In these figures, the motor was analyzed magneto-statically for magnet heights from

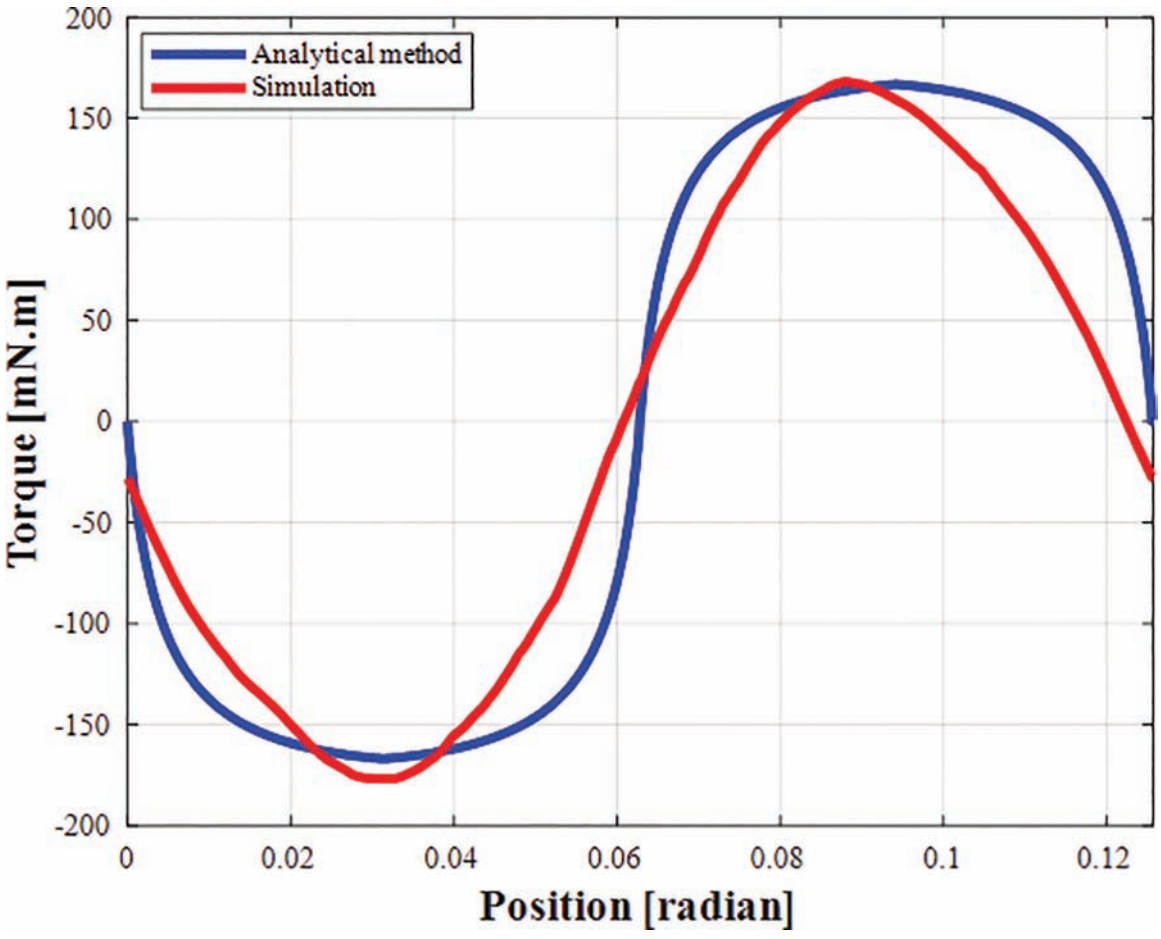

Figure 7: Comparison between torque curves in analytical and numerical simulation models.

9 mm to 21 mm. As illustrated, the magnetic flux density in the teeth is relatively uniform at about 1 Tesla.

As can be seen in Figures 10B and 10C, the only effect that the magnet height has on the motor is the increase in flux density at the upper or lower end of the rotor, but this effect is negligible at the air gap because the magnetic flux must still pass the same distance to reach this area.

This trend is also the same when the motor is not excited. As it is represented in Figure 11, the motor produces very small torque levels when the rotor is rotated which is called the motor cogging torque. This torque for different magnet heights is almost the same which again proves that the magnet height does not affect the motor performance.

b. Magnet diameter

It has been shown in the previous section that the motor is not sensitive to the magnet height, but it seems that the performance of the motor is affected by the magnet diameter as the magnetic flux in the teeth varies with the variations in the magnet edge distance from the rotor teeth. This effect is illustrated in Figure 12. In Figures 12 and 13, all the parameters are the same as in Table 1 except for the magnet diameter.

As can be seen in Figure 12, despite the excitation of the coils with a current of 1.5 A, the motor torque has changed significantly with a slight change in the magnet diameter, indicating a high sensitivity of the motor to the magnet diameter. In Figure 13, the variations of the magnetic flux density on the rotor teeth caused by two magnets of 20.8 mm and 10.8 mm in diameter can be seen clearly.

By comparing Figures 13A and 13B, it can be seen clearly that with increasing magnet diameter, the flux density increases dramatically which is the result of the magnet near the rotor teeth, and consequently, the motor torque will increase dramatically.

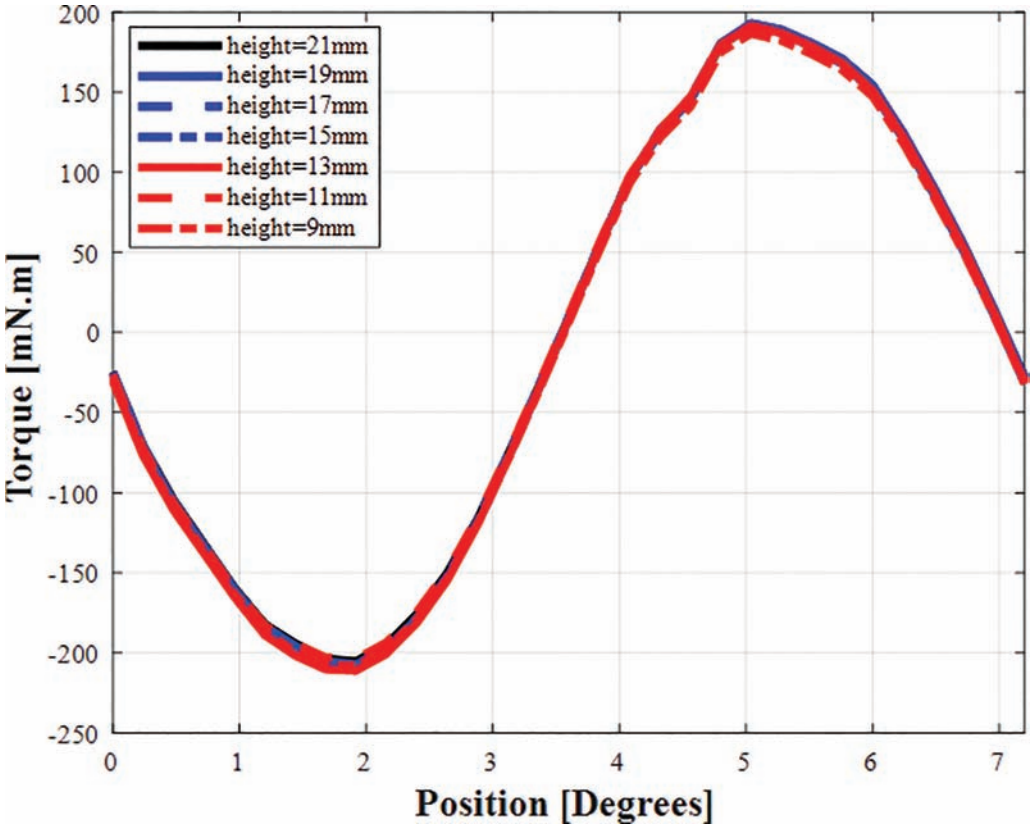

Figure 8: A sample meshing used for 3D FEM analysis. FEM, finite element method.

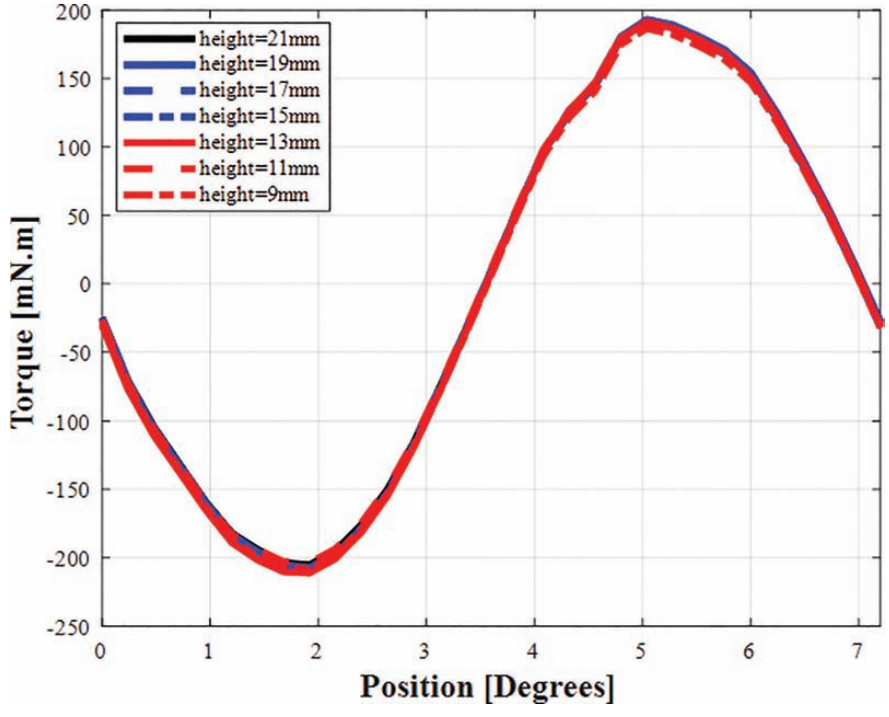

Figure 9: Motor torque for different magnet heights.

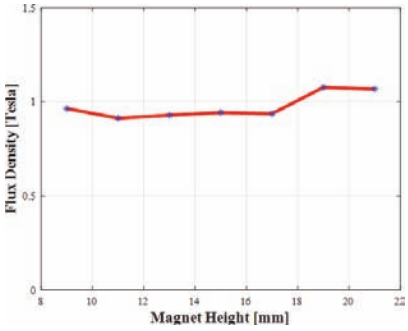

(A)

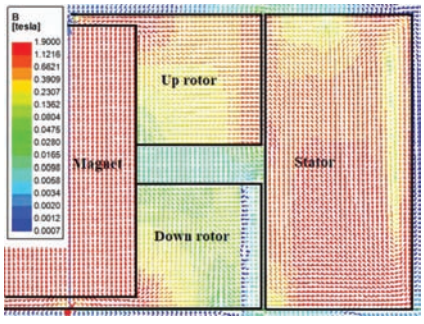

(B)

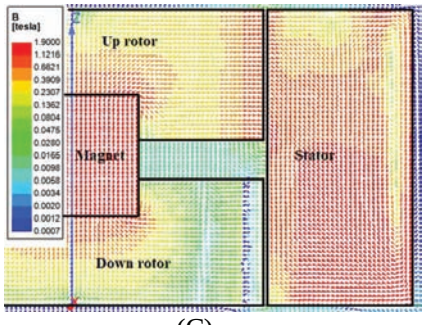

(C)

Figure 10: Flux density, (A) magnet heights 9–21 mm, (B) magnet height is 21 mm, (C) magnet height is 9 mm.

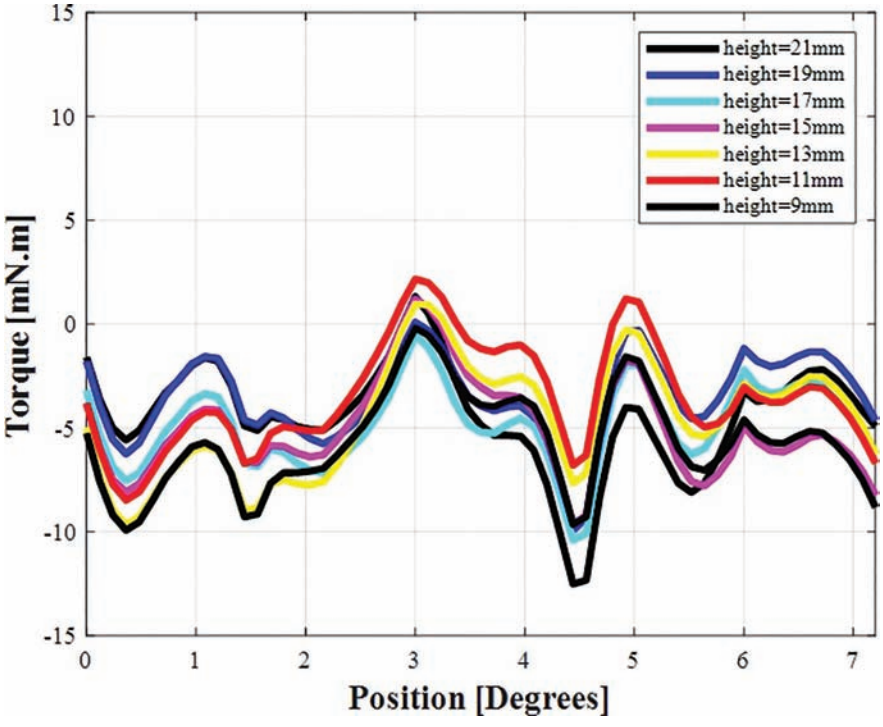

Figure 11: Motor torque for magnet heights from 21 mm to 9 mm when the stator coils are not excited.

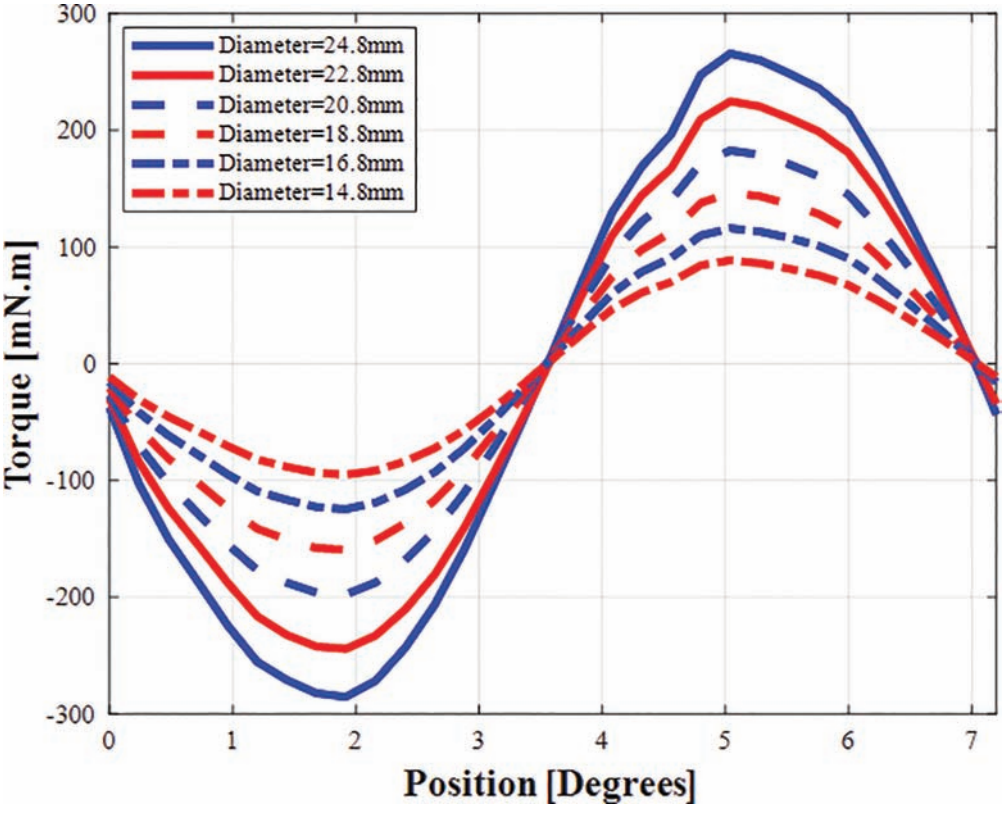

Figure 12: Motor torque for different magnet diameters.

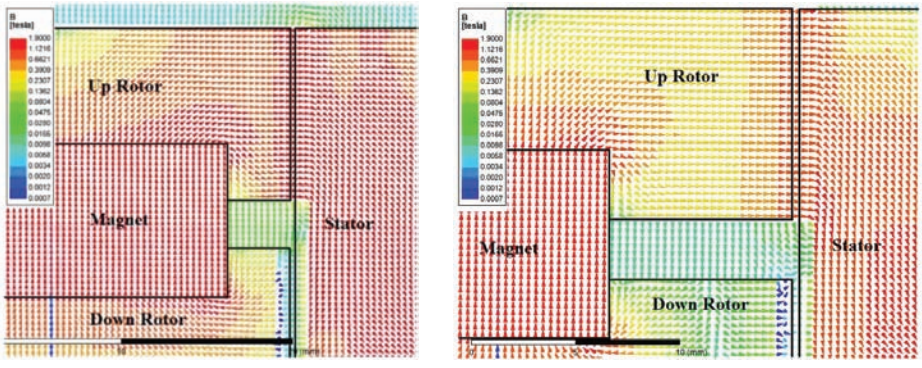

(A) (B)

Figure 13: Flux density, (A) magnet diameter is 20.8 mm and (B) magnet diameter is 10.8 mm.

For different magnet diameters, this trend is also the same when the motor is not excited.

As represented in Figure 14, although the motor-produced torque is very small, it alters for different magnet diameters; and as the magnet diameter shrinks, the produced cogging torque leads to a straight line.

c. Magnet flux density

The magnet type and the magnetic flux density created by it play an important role in the amount of torque produced by the stepper motor. This is due to the flux density increase or decrease in the air gap between the rotor and stator teeth. Studies have shown that while the motor core is not saturated, its

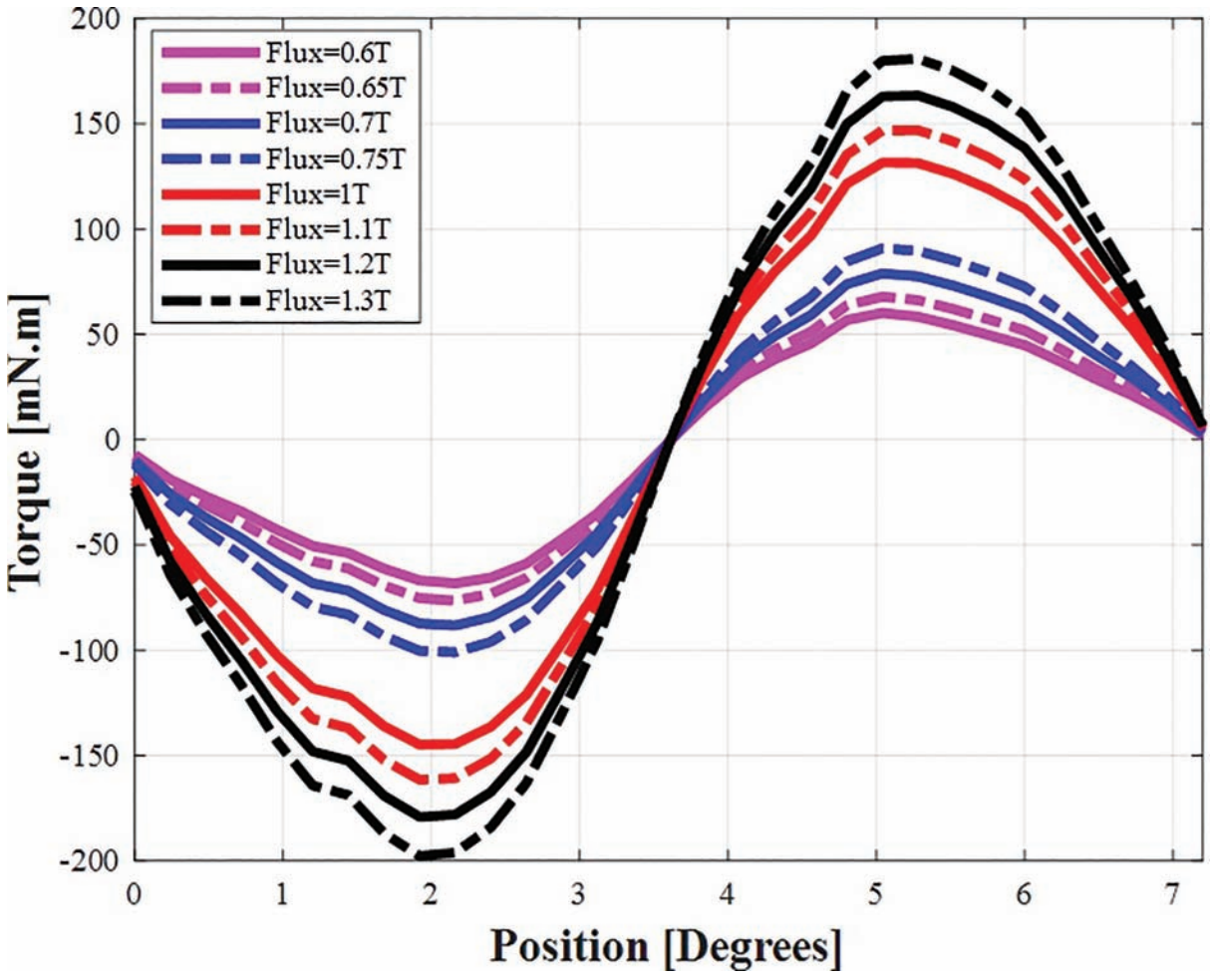

Figure 14: Motor torque for magnet diameters from 29.8 mm to 24.8 mm when the stator coils are not excited.

torque changes linearly with flux density variations. Therefore, the sensitivity of the motor is proportional to the changes in this parameter. In Figure 15, the performance of the motor based on the magnetic flux density changes can be seen vividly. In this graph, the motor is excited with 1.5 A. To change the magnetic flux density in the rotor, the rotor magnet has been replaced with an electric magnet, and with different excitations, the magnetic flux densities shown in this figure are produced. In this simulation, all the other parameters are the same as in Table 1.

d. Air gap

One of the most effective parameters on motor performance is the air gap. This parameter is such influential that by decreasing it from 0.1 mm to 0.05 mm the motor torque increases from about 180 N/mm to about 300 mN/m. This is due to its direct impact on the amount of flux density that passes through the motor components. The shorter the air gap, the less the resistance to magnetic flux. However, by decreasing the air gap, the motor fabrication problems increase. Figure 16 shows the effect of this parameter on flux distribution and flux density on the teeth and the air gap. In Figure 17, the torque curve can be seen for several air gaps with 1.5 A excitation in stator coils. In these simulations, all the parameters are the same as in Table 1 except for the air gap distance.

e. Number of wire-turns per coil

One of the factors affecting the performance and power of the motor is the number of wire-turns per coil. As can be seen in Figure 18, with a reduction of

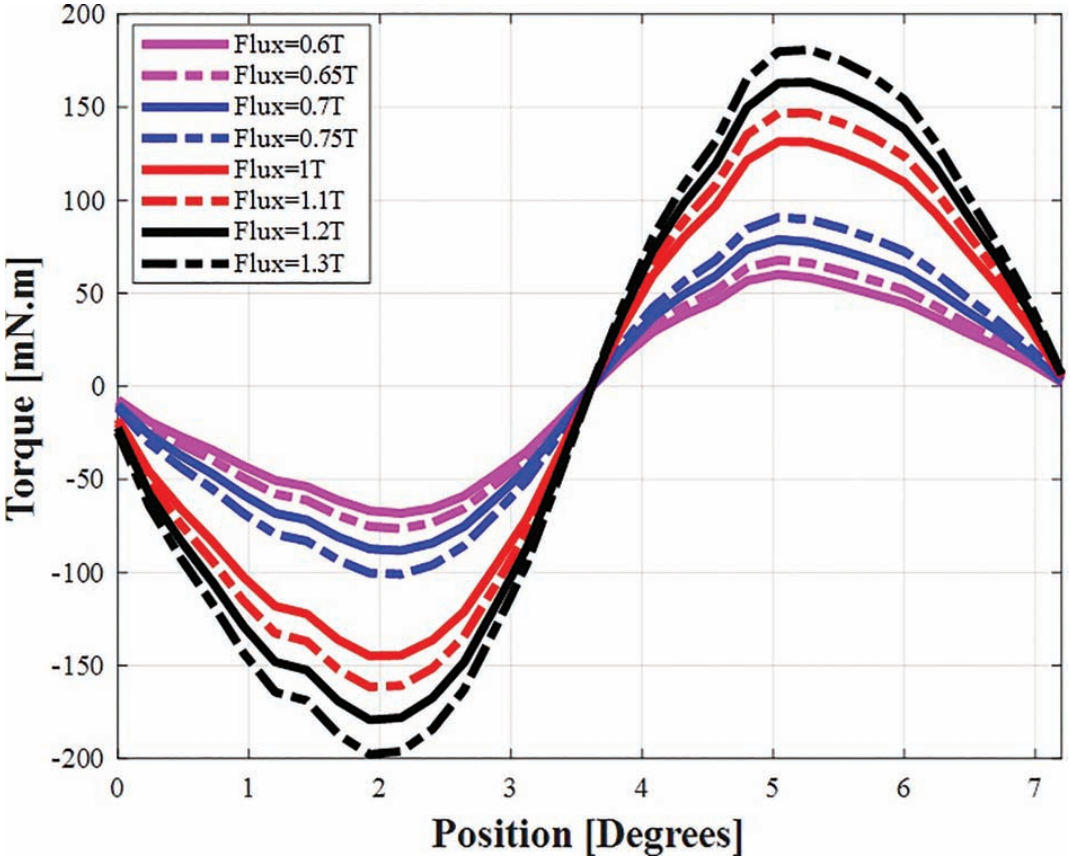

Figure 15: Motor torque for different magnetic flux densities.

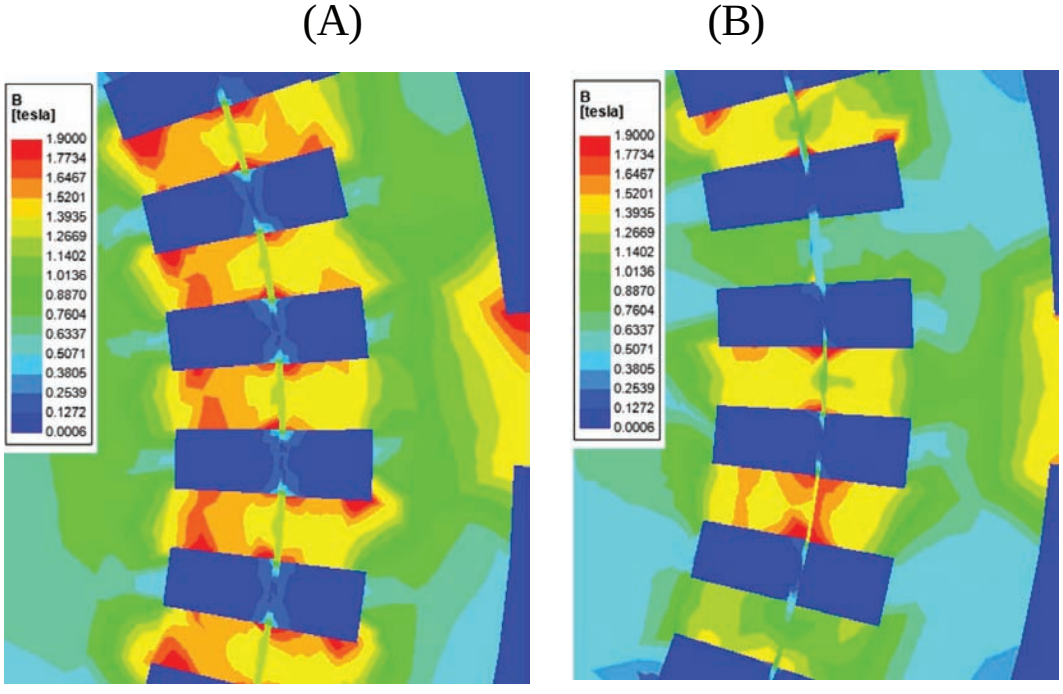

Figure 16: Flux density distribution for two different air gaps- (A) 0.1 mm and (B) 0.05 mm.

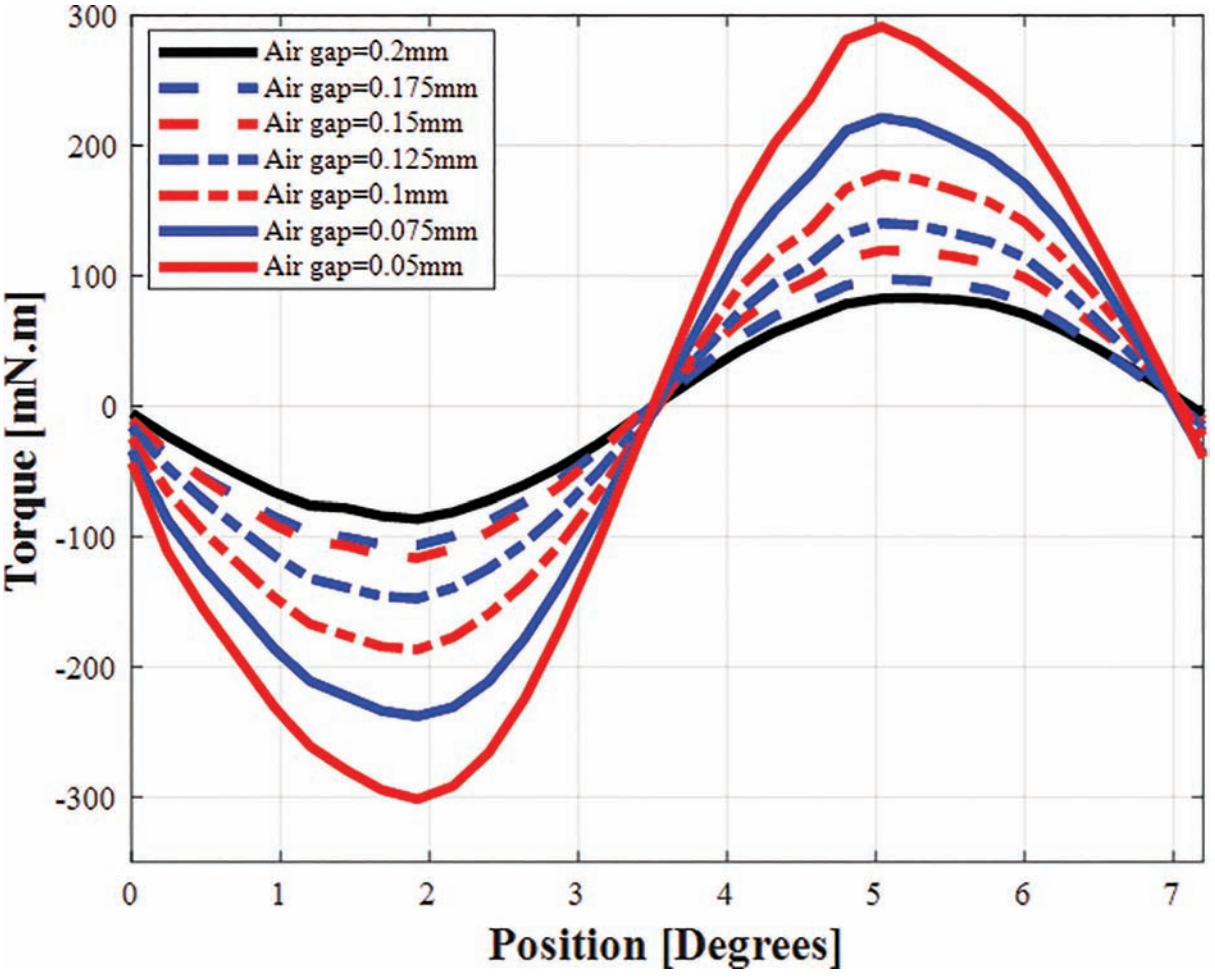

Figure 17: Motor torque for different air gaps.

two turns of wire per coil, the motor torque declines 20 N/mm which means that by reducing the number of turns to 96%, the motor torque also reduces to 96%. In this diagram, because the motor is excited with 1.5 A, it is still very far from the saturation situation even with 33 turns of wire. In this simulation, all the parameters are the same as in Table 1 except for the wire-turns number.

f. Teeth depth in the rotor and stator

The teeth in the rotor and stator are very effective on motor performance. The proper depth of the teeth improves the sinusoidal waveform of the torque and improves symmetry for the positive and negative peak points of the torque curve. Also, it can improve the motor's torque output. In Figures 19–21, the influence of change in the rotor, stator, and both teeth depth on the torque curve is illustrated respectively. In these simulations, all the parameters are the same as in Table 1 except for the rotor and the stator depth.

g. Teeth width

The teeth width, as well as their depth, has a great influence not only on the overall behavior of the motor and its output torque but also on the torque waveform shape in terms of symmetry. Therefore, it can be said that the motor is highly sensitive to this parameter. In the motor understudy, the teeth width is 3.6°, but as shown in Figure 22, this angle is not quite optimal and the angles from 3.1° to 2.6° have the best waveforms. In this simulation, all the parameters are the same as in Table 1 except for the teeth width of the rotor and the stator.

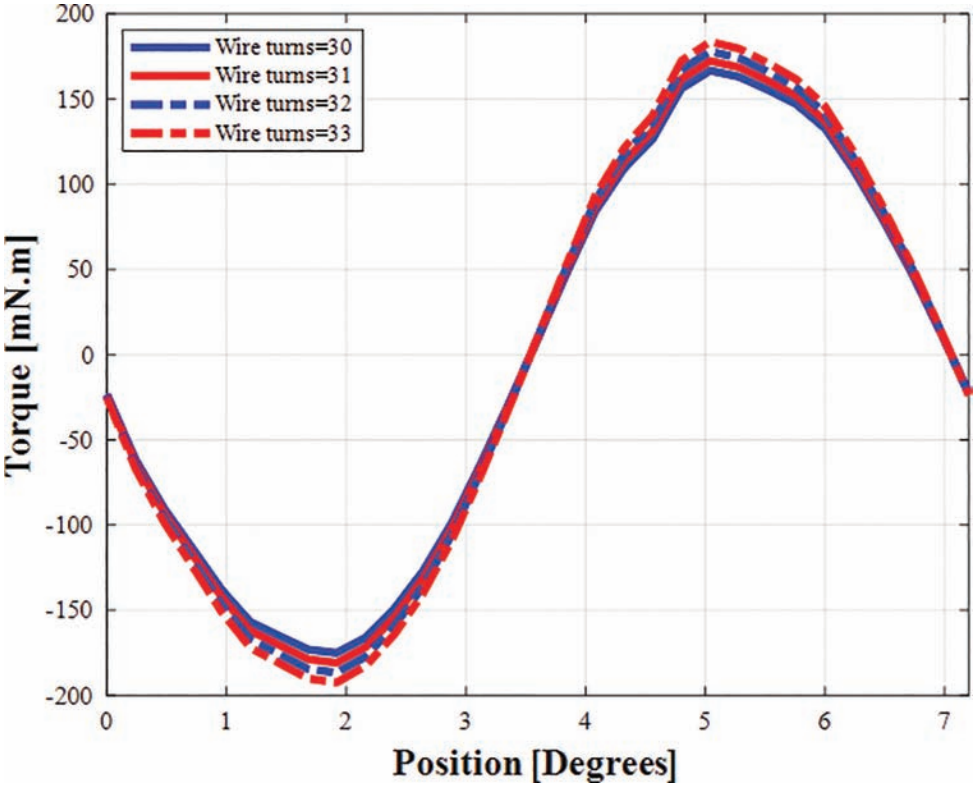

Figure 18: Motor torque for different wire-turns in stator coils.

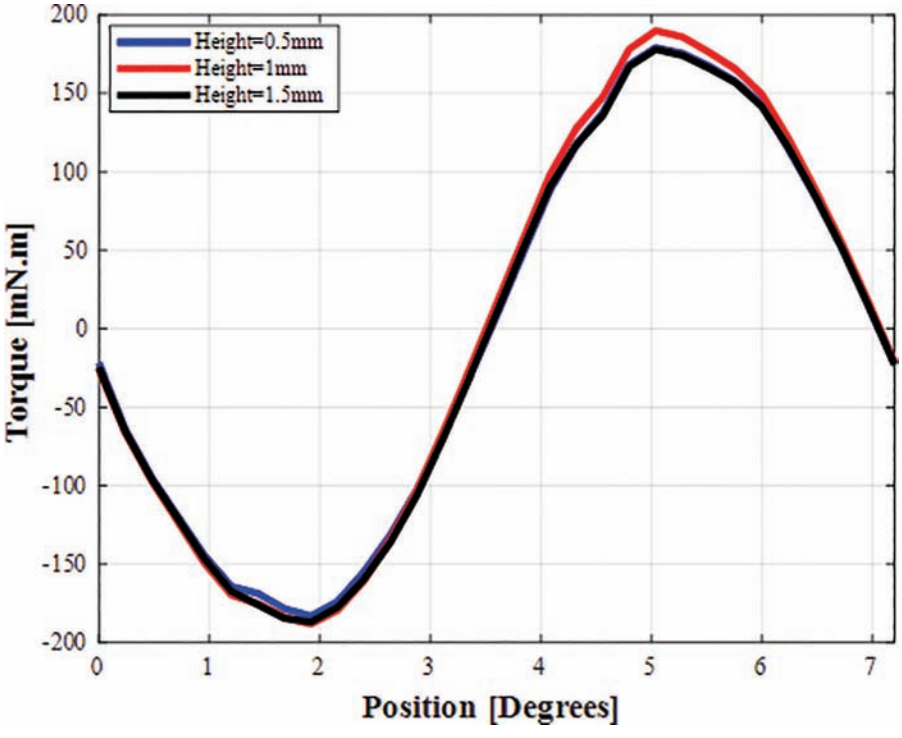

Figure 19: Rotor teeth depth influence on motor torque.

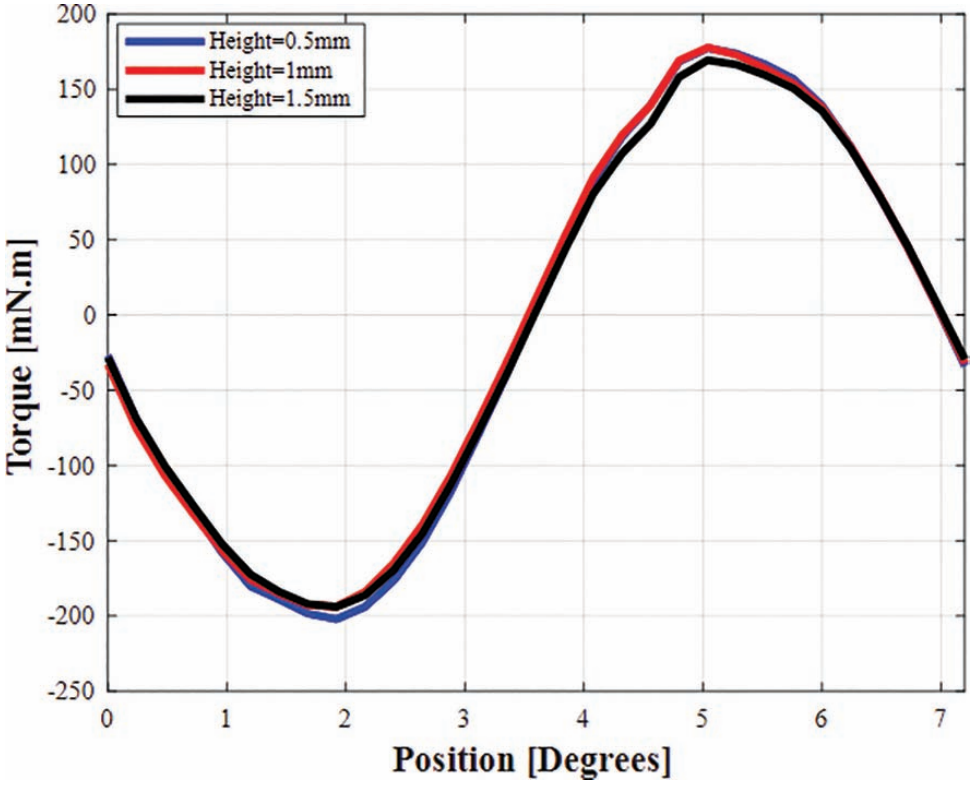

Figure 20: Stator teeth depth influence on motor torque.

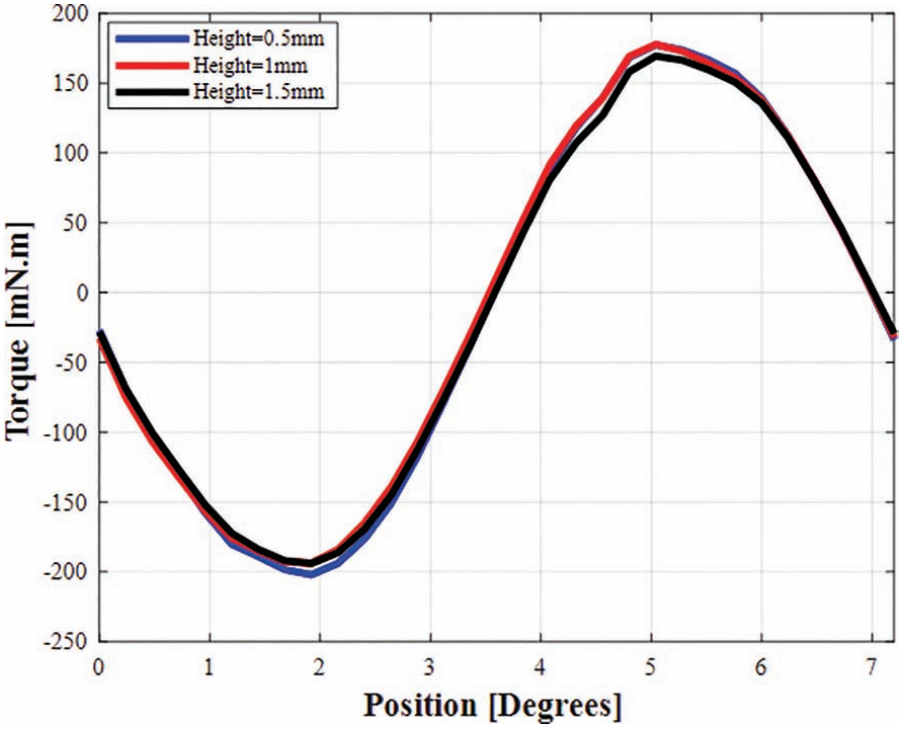

Figure 21: Both rotor and stator teeth depth influence on motor torque.

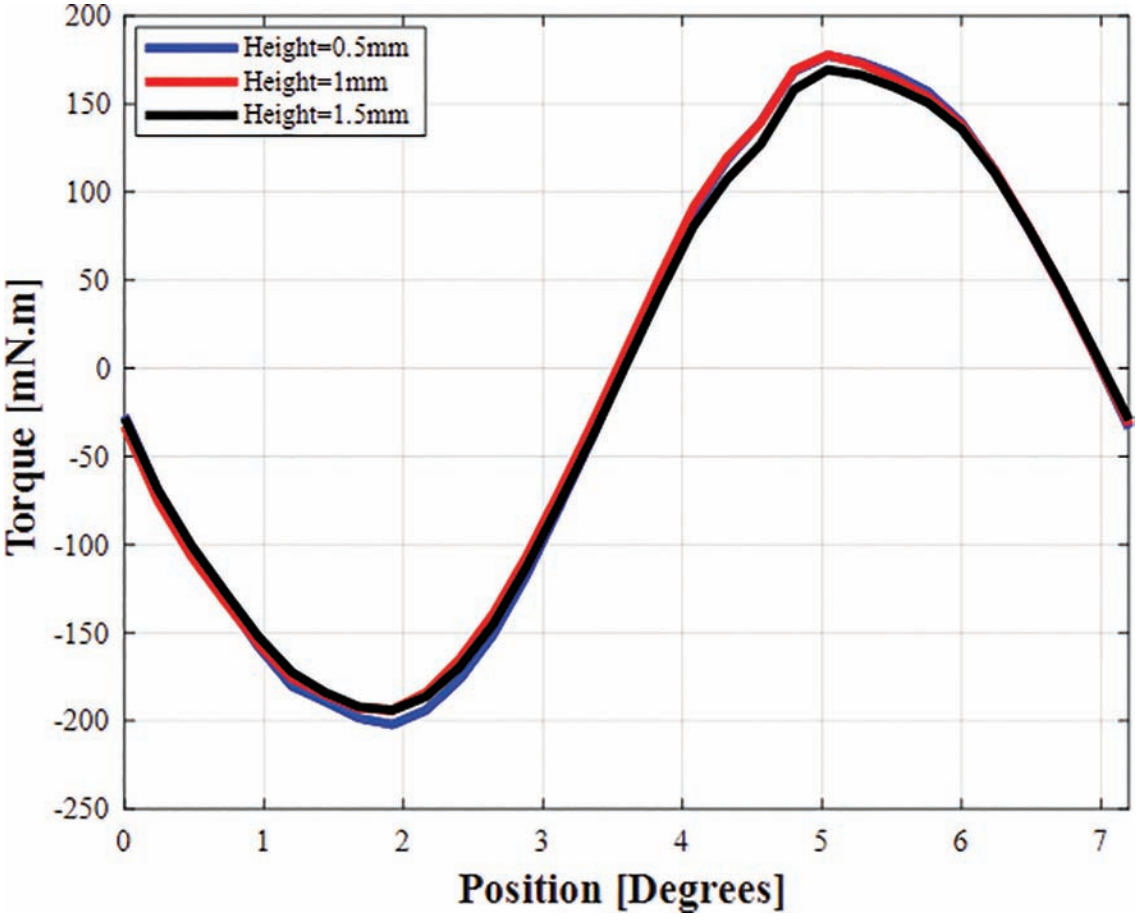

Figure 22: Motor torque for different teeth width.

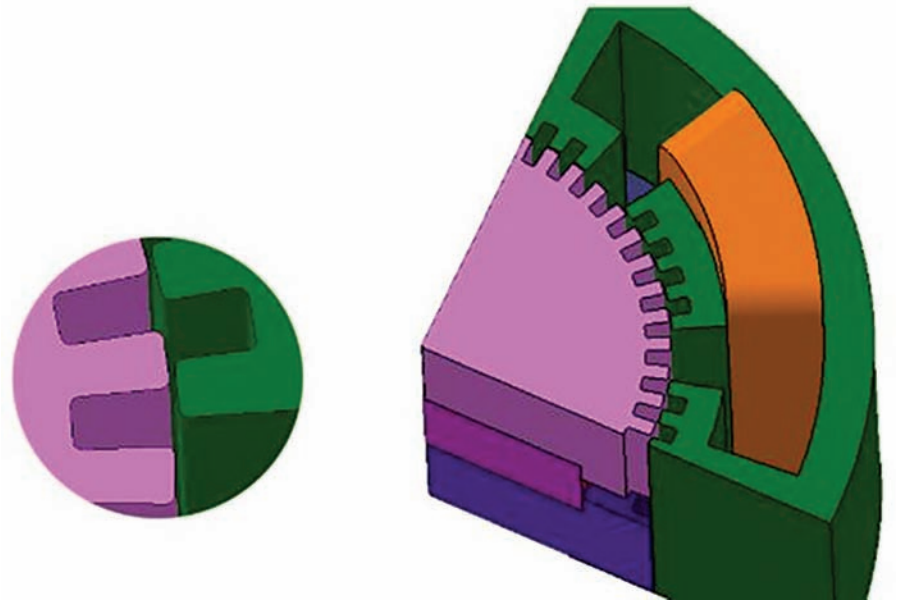

Figure 23: Fillet on the teeth edges.

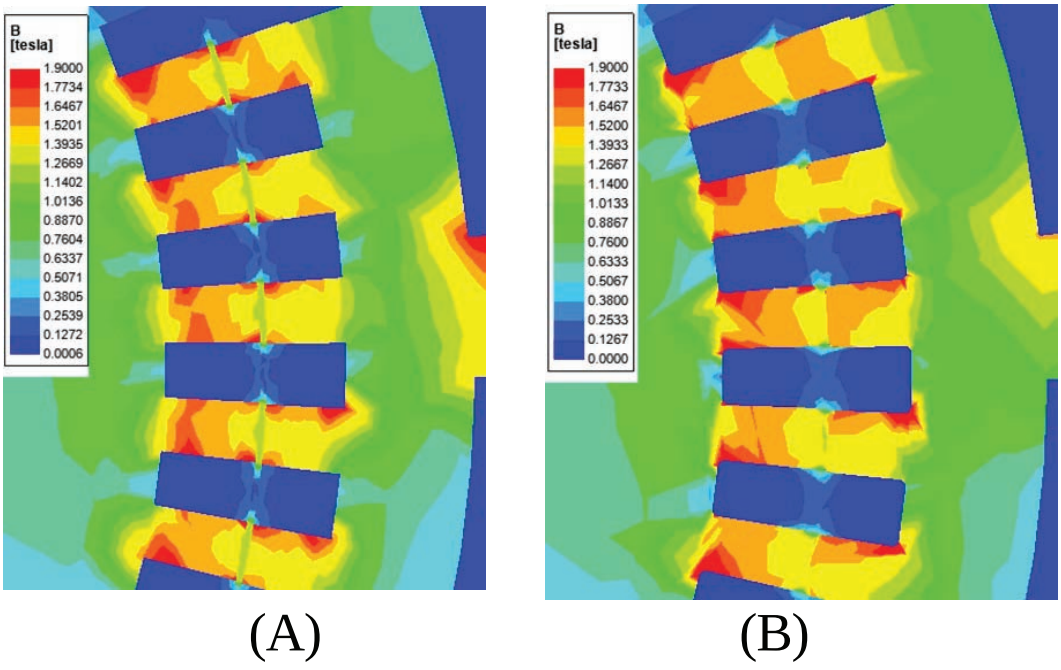

Figure 24: The effect of teeth fillet on flux distribution, (A) Fillet radius = 0 mm and (B) Fillet radius = 0.125 mm.

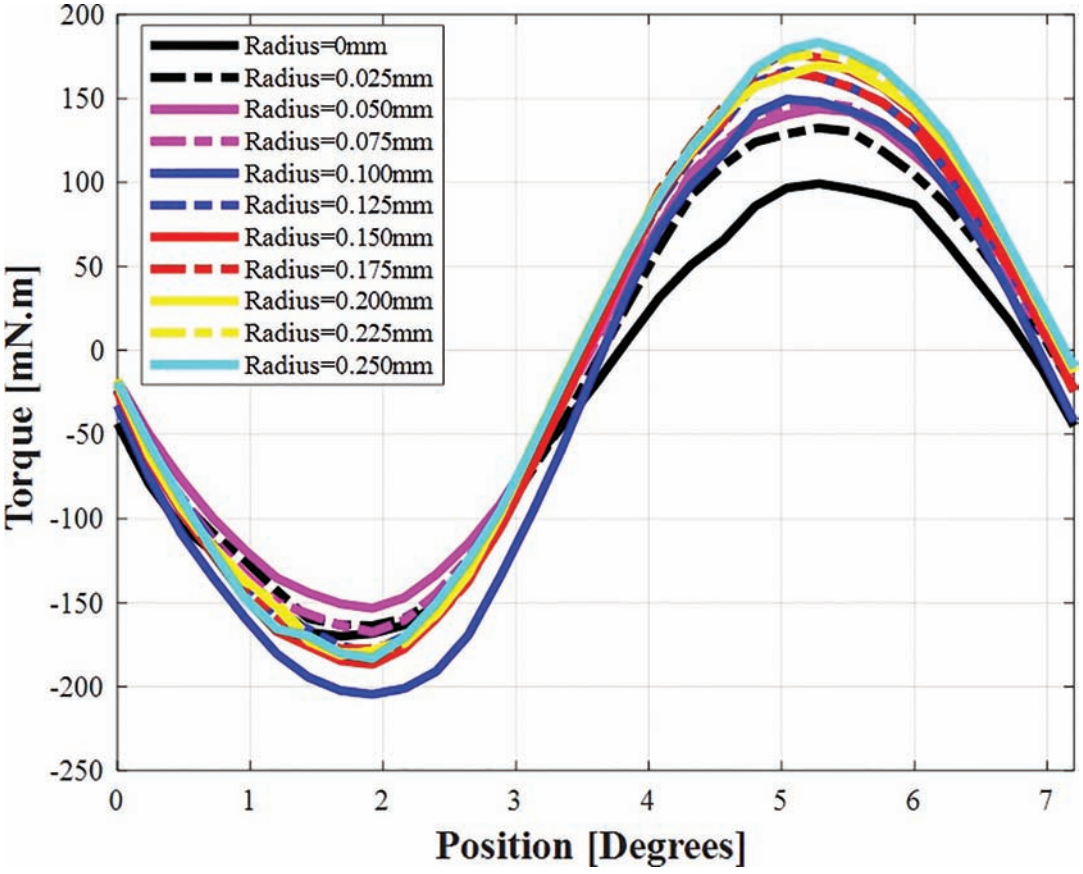

Figure 25: Motor torque with different fillet radiuses.

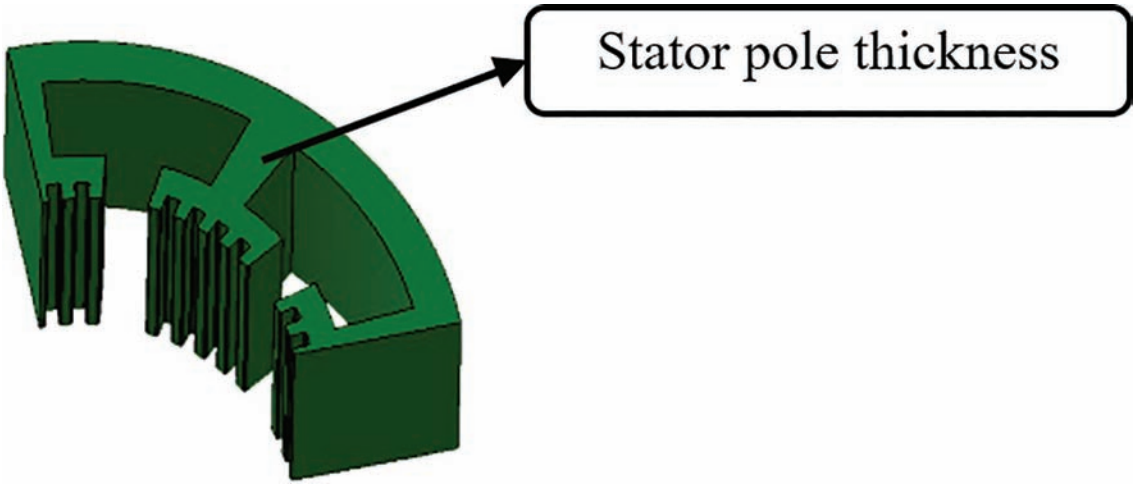

Figure 26: Stator pole thickness.

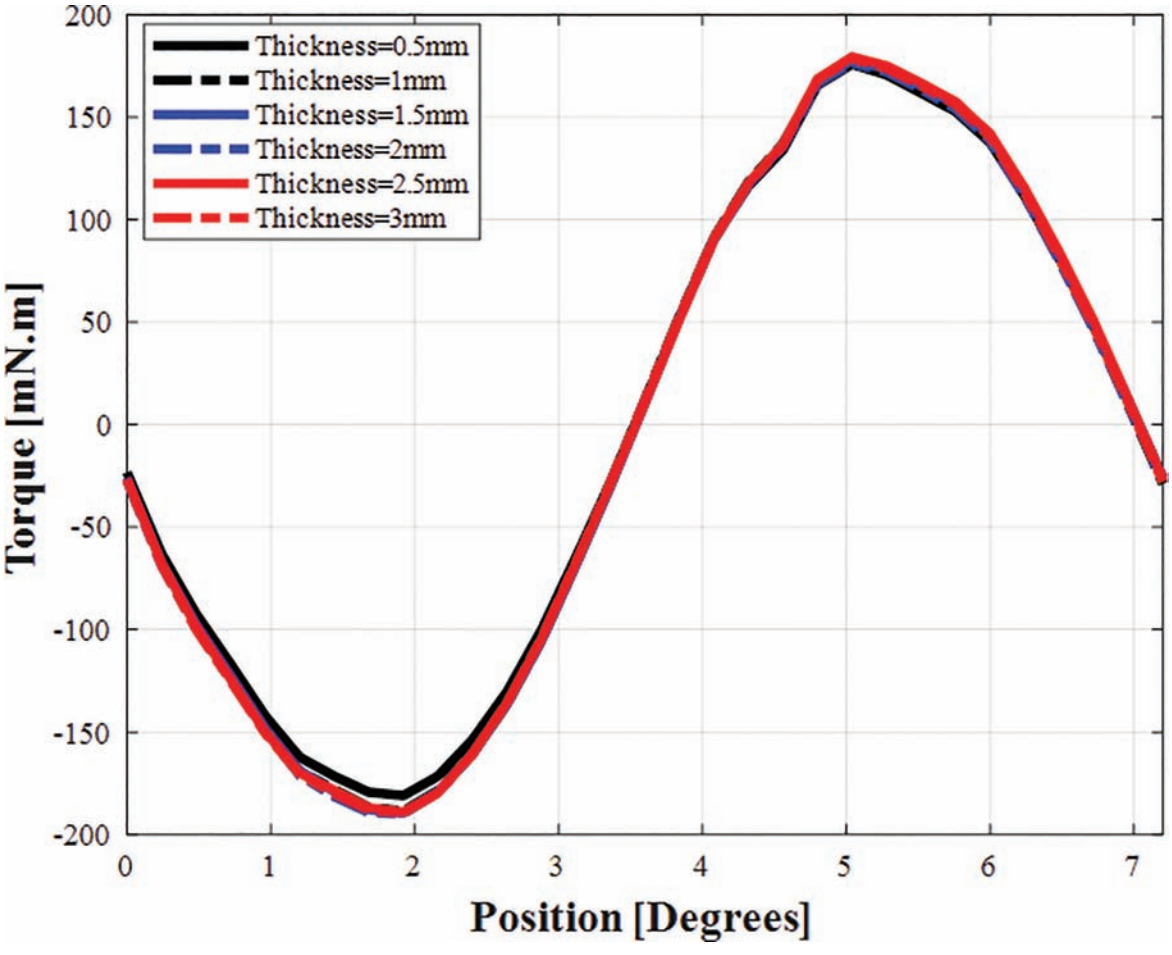

Figure 27: Stator pole thickness influence.

h. Teeth fillet

The fillet radius on the edge of the rotor and stator teeth (as shown in Figure 23) has a great influence on motor behavior. This effect is similar to the effect of the depth of the rotor and stator teeth, except that it is much more intense and the motor is more sensitive to it. This is due to its effect on the distribution of magnetic flux passing the air gap. When the edges of the teeth are sharp and without fillets, in those sharp points flux concentration is created resulting in saturation on those areas. Thus, this phenomenon affects the flux density on the air gap significantly. Moreover, the fillet radius is effective and important as well.

In Figure 24, the discontinuity of the flux in the air gap for the sharp teeth situation, and its consistency and uniformity for the filleted teeth can be seen clearly. In addition, in Figure 25, the effect of the fillet with different radiuses is illustrated. In these simulations, all the parameters are the same as in Table 1 except for the teeth fillet radius.

i. Stator pole thickness

Stator poles are used to place the teeth and are essential for the transmission of magnetic flux (Figure 26). The thickness of this part seemed to play a critical role in the motor performance; however, studies showed that the motor was not sensitive to this parameter and therefore, the thickness of this section on the torque curve is negligible. Figure 27 illustrates it clearly. In this simulation, all the parameters are the same as in Table 1 except for the stator pole thickness.

V. Conclusion

This study focused on analyzing the torque of HSMs and investigating their sensitivity to different parameters. A real HSM was first modeled and simulated. After obtaining the motor parameters, the simulated model was compared with the actual HSM to ensure its accuracy. The simulation results were then compared with the analytical model to evaluate these two methods and investigate the influence of various parameters on the output torque waveform.

The study found that the simplifications made in the analytical model caused minor errors, rendering the waveform not entirely accurate. However, these errors did not affect the desired result, which is the maximum produced holding torque. Finally, the effects of different motor parameters were investigated using the 3D FEM method.

The results showed that HSMs are most sensitive to parameters such as magnet diameter, magnetic flux density, air gap, number of wire-turns in the coils, teeth width, and teeth fillet. Small changes in these parameters significantly affect motor performance. In contrast, parameters such as magnet height and stator pole thickness have minimal impact on motor performance, allowing flexibility in designing new HSM motors with higher torque and power density.

References

[1] Paul P Acarnley. *Stepping motors: a guide to theory and practice*. Number 63. Iet, 2002.

[2] Paolo Visconti, Patrizio Primiceri, R De Fazio, and A Lay Ekuakille. A solar-powered white led-based uv-vis spectrophotometric system managed by pc for air pollution detec- tion in faraway and unfriendly locations. *International Journal on Smart Sensing and Intelligent Systems*, 10(1):1–31, 2017.

[3] Hirokazu Nosato, Nobuharu Murata, Tatsumi Furuya, and Masahiro Murakawa. Auto- matic adjustment for laser systems using a stochastic binary search algorithm to cope with noisy sensing data. *International Journal on Smart Sensing and Intelligent Systems*, 1(2):512–533, 2008.

[4] Pengfei Gui, Liqiong Tang, and Subhas Mukhopadhyay. A novel design of anti-falling mechanism for tree pruning robot. In *2015 IEEE 10th conference on Industrial Electronics and Applications (ICIEA)*, pages 812–816. IEEE, 2015.

[5] Pengfei Gui, Liqiong Tang, and Subhas Mukhopadhyay. A novel robotic tree climbing mechanism with anti-falling functionality for tree pruning. *Journal of Mechanisms and Robotics*, 10(1):014502, 2018.

[6] Pengfei Gui, Liqiong Tang, and Subhas Mukhopadhyay. Tree pruning robot tilting control using fuzzy logic. In *2017 Eleventh International Conference on Sensing Technology (ICST)*, pages 1–5. IEEE, 2017.

[7] Jose Cornejo, S Barrera, CA Herrera Ruiz, F Gutierrez, MO Casasnovas, Leonardo Kot, MA Solis, R Larenas, F Castro-Nieny, MR Arbulu´ Saavedra, et al. Industrial, collaborative and mobile robotics in latin america: Review of mechatronic technologies for advanced automation. *Emerging Science Journal*, 7(4):1430–1458, 2023.

[8] Elanda Fikri, Irfan A Sulistiawan, Agus Riyanto, and Aditiyana Eka Saputra. Neutraliza- tion of acidity (ph) and reduction of total suspended solids (tss) by solar-powered electro- coagulation system. *Civil Engineering Journal*, 9(5):1160–1172, 2023.

[9] Luis A Morales, Paul Fabara, and David Fernando Pozo. An intelligent controller based on lamda for speed control of a three-phase inductor motor. *Emerging Science Journal*, 7(3):676–690, 2023.

[10] LK Lai and TS Liu. Design of auto-focusing modules in cell phone cameras. *International Journal on Smart Sensing and Intelligent Systems*, 4(4):568–582, 2011.

[11] MK Jenkins, D Howe, and TS Birch. An improved design procedure for hybrid stepper motors. *IEEE transactions on magnetics*, 26(5):2535–2537, 1990.

[12] Dae-Sung Jung, Seung-Bin Lim, Ki-Chan Kim, JoonSeon Ahn, Sung-Chul Go, Yeoung- Gyu Son, and Ju Lee. Optimization for improving static torque characteristic in permanent magnet stepping motor with claw poles. *IEEE transactions on magnetics*, 43(4):1577–1580, 2007.

[13] Takashi Kosaka and Nobuyuki Matsui. Simple nonlinear magnetic analysis for three-phase hybrid stepping motors. In *Conference Record of the 2000 IEEE Industry Applications Conference. Thirty-Fifth IAS Annual Meeting and World Conference on Industrial Appli- cations of Electrical Energy (Cat. No. 00CH37129)*, volume 1, pages 126–31. IEEE, 2000.

[14] Nobuyuki Matsui, Makoto Nakamura, and Takashi Kosaka. Instantaneous torque analysis of hybrid stepping motor. *IEEE transactions on Industry Applications*, 32(5):1176–1182, 1996.

[15] EVC Sekhara Rao and PVN Prasad. Torque analysis of permanent magnet hybrid stepper motor using finite element method for different design topologies. *International Journal of Power Electronics and Drive Systems*, 2(1):107, 2012.

[16] Cornelia Stuebig and Bernd Ponick. Comparison of calculation methods for hybrid step- ping motors. *IEEE Transactions on Industry Applications*, 48(6):2182–2189, 2012.

[17] Seong Gu Kang and Dennis K Lieu. Torque analysis of combined 2d fem and lumped parameter method for a hybrid stepping motor. In *IEEE International Conference on Electric Machines and Drives, 2005.*, pages 1199–1203. IEEE, 2005.

[18] Ki-Chae Lim, Jung-Pyo Hong, and Gyu-Tak Kim. Characteristic analysis of 5-phase hybrid stepping motor considering the saturation effect. *IEEE transactions on magnetics*, 37(5):3518–3521, 2001.

[19] M Bendjedia, Y Ait-Amirat, B Walther, and A Berthon. Sensorless control of hybrid stepper motor. In *2007 European Conference on Power Electronics and Applications*, pages 1–10. IEEE, 2007.

[20] Weijie Lin and Zhuo Zheng. Simulation and experiment of sensorless direct torque control of hybrid stepping motor based on dsp. In *2006 International Conference on Mechatronics and Automation*, pages 2133–2138. IEEE, 2006.

[21] Mark Butcher, Alessandro Masi, Ricardo Picatoste, and Alessandro Giustiniani. Hybrid stepper motor electrical model extensions for use in intelligent drives. *IEEE Transactions on Industrial Electronics*, 61(2):917–929, 2013.

[22] Hoang Le-Huy, Patrice Brunelle, and Gilbert Sybille. Design and implementation of a ver- satile stepper motor model for simulink's simpowersystems. In *2008 IEEE International Symposium on Industrial Electronics*, pages 437–442. IEEE, 2008.

[23] Amir Mehdi Yazdani, Ahmadreza Ahmadi, Salinda Buyamin, Mohd Fua'ad Rahmat, Far- shad Davoudifar, and Herlina Abd Rahim. Imperialist competitive algorithm-based fuzzy pid control methodology for speed tracking enhancement of stepper motor. *International Journal on Smart Sensing and Intelligent Systems*, 5(3):717–741, 2012.

[24] Binglin Lu, Yanliang Xu, and Xin Ma. Design and analysis of a novel stator-permanent- magnet hybrid stepping motor. *IEEE Transactions on Applied Superconductivity*, 26(7):1– 5, 2016.

[25] J Kavitha and B Umamaheswari. Analysis of a novel disc-type hybrid stepper motor with field circuit model. *Sādhanā*, 44(5):1–12, 2019.

[26] Mohammadreza Hojati, Amir Baktash, Ali Jabbari, and Ehsan Soury. An improved struc- ture for hybrid stepper motors to increase the torque density. *Iranian Journal of Science and Technology, Transactions of Electrical Engineering*, 46(4):1223–1232, 2022.

[27] Mohammadreza Hojati and Amir Baktash. Hybrid stepper motor with two rows of teeth on a cup-shaped rotor and a two-part stator. *Precision Engineering*, 73:228–233, 2022.

[28] Mohammadreza Hojati and Amir Baktash. Design and fabrication of a new hybrid stepper motor with significant improvements in torque density. *Engineering Science and Technol- ogy, an International Journal*, 2021.